Applied Thermal Engineering 125 (2017) 425–431

Contents lists available at ScienceDirect

Applied Thermal Engineering

journal homepage: www.elsevier.com/locate/apthermeng

Research Paper

Experimental prototype and simulation optimization of micro-radial milliwatt-power radioisotope thermoelectric generator

Kai Liu [a], Yunpeng Liu [a,b], Zhiheng Xu [a], Zhengrong Zhang [a], Zicheng Yuan [a], Xiao Guo [a], Zhangang Jin [a], Xiaobin Tang [a,b,*]

[a] Department of Nuclear Science and Engineering, Nanjing University of Aeronautics and Astronautics, Nanjing 210016, China
[b] Jiangsu Key Laboratory of Material and Technology for Energy Conversion, China

HIGHLIGHTS

- A micro-radial radioisotope thermoelectric generator is manufactured and tested.
- The simulated performance of the RTG are compared with the experimental value.
- Performance characteristics were determined in different sizes and numbers.
- The designed RTG is expected to be a reliable space power supply for MEMS.

ARTICLE INFO

Article history:
Received 18 March 2017
Revised 6 June 2017
Accepted 3 July 2017
Available online 4 July 2017

Keywords:
Bismuth telluride
Energy conversion
COMSOL
MEMS
Radioisotope thermoelectric generator

ABSTRACT

To satisfy the flexible power demand of the low power dissipation devices in the independent space electric system, a micro-radial milliwatt-power radioisotope thermoelectric generator (RTG) was prepared and optimized in this research. The overall geometrical dimension of the RTG in the experiment was 65 mm (diameter) × 40 mm (height). The RTG, which was built and tested using simulated radioisotope source, eventually obtained an open-circuit voltage of 92.72 mV, an electric power of 149.0 μW, and an energy conversion efficiency of 0.015% at the ambient temperature of 293.15 K and heat source power from 0.1 W to 1 W. On the basis of the structure used in the experiment, the length and cross-sectional area of the thermoelectric leg and the number of thermoelectric modules were effectively optimized through the COMSOL Multiphysics. With the optimized length of 35 mm and cross-sectional area of 1.2 mm^2, the RTG with four thermoelectric modules achieved a 15.8 mW output power under 1 W heat source power. The maximum conversion efficiency calculated using COMSOL code increased to 1.58%. According to the optimized electrical output, the micro-radial RTG is expected to be a reliable space power supply for micro components and could satisfy the low power requirements of space missions.

1. Introduction

With the development of space technology, the requirements of various space vehicles have increased in terms of lifetime, reliability and environmental adaptability of power systems, especially for deep space exploration [1,2]. Solar cells are unsuitable for low-light environments and high-capacity batteries, such as lithium batteries and fuel cells cannot satisfy the long-term electricity demand of space devices [3]. As a device that converts the decay heat of radioactive isotopes into electrical energy, the radioisotope thermoelectric generator (RTG) has numerous advantages, such as high reliability, long lifetime and minimal environmental impact [4]. Therefore, it is widely considered as one of the most ideal energy supply devices for deep space exploration [5–7].

Space missions for environmental exploration and scientific experiments are constantly being launched. Therefore, the demands of small scientific instruments and micro-electro-mechanical systems (MEMS) for portable power supply are also increasing [8,9]. To achieve greater flexibility and convenience in performing space missions and to satisfy the conditional restrictions, such as aircraft load and space volume simultaneously, RTGs are likely to develop toward the miniaturization target [10–13]. Weber et al. manufactured a coiled-thermoelectric power generator with thousands of thin-film thermocouples that are electrically in series; their work achieved a high output voltage, but the energy conversion efficiency was low because of the unidirectional heat

* Corresponding author at: Department of Nuclear Science and Engineering, Nanjing University of Aeronautics and Astronautics, Nanjing 210016, China.
E-mail address: tangxiaobin@nuaa.edu.cn (X. Tang).

http://dx.doi.org/10.1016/j.applthermaleng.2017.07.022
1359-4311/

Nomenclature

A_1	the heat-receiving area, mm^2
C	the Stefan–Boltzmann constant
F_{12}	the view factor
h	the convective heat transfer coefficient, $W/(m^2 \cdot K)$
J	the current density of a pair of PN leg
L	the length of a single P-type or N-type leg, mm
n	number of thermocouples
P_{out}	the output power of the RTG, mW
P_{max}	the maximum output power of the RTG, mW
P_h	the heat source power released by the radiation source, W
q	the heat flux of a pair of PN leg, W/m^2
q_0	the convective heat flux
Q	the energy accumulation of a pair of PN leg
Q_{rad}	the net heat radiation from surface to surface, W/m^2
r	the internal resistance in the RTG, Ω
R	the external load resistance in the RTG, Ω
S	the cross-sectional area of a single P-type or N-type leg, mm^2
V	the output voltage of the RTG, V
V_{oc}	the open-circuit voltage of the RTG, V
ZT	the figure of merit
ΔT	Temperature difference of both hot and cold side of RTG
σ	electrical conductivity, S/m
α	seebeck coefficient, V/K
κ	thermal conductivity, W/(m·K)
η	the conversion efficiency
ε	the emissivity coefficient

transmission [14]. Whalen et al. designed a cylindrical micro thermoelectric battery with an energy conversion efficiency of 0.3% due to its spoke design, but its structure could be further optimized [15]. Some researchers have also studied the optimization of thermoelectric devices. Wang et al. built a numerical modeling of thermoelectric device with coupling of temperature field and electric potential field, and in-depth study of optimized size parameters, material properties, and the heat loss were considered integrally [16–18]. Chen et al. adopted the Taguchi method to effectively optimize performance of a thermoelectric generator, and a solar thermoelectric generator at three different geometric types was also simulated [19–20]. With regard to RTGs, worthy research subjects include effectively improving the performance output and conversion efficiency and the in-depth exploration of the relationship between the electrical properties and the structure size of RTGs through theoretical analysis and experiments [21,23]. Therefore, in response to the low power demand of certain space devices, this work presents the structure design, experimental preparation and performance testing of a micro-radial RTG. The finite element analysis method is used to optimize the RTG's size and structure, and the optimized RTG is proposed to provide stable power for space devices [24,25].

2. Experiment and simulation

2.1. Structure design

Fig. 1 shows the three-dimensional model of the radial RTG. The middle part of the RTG is a cylindrical radioisotope source, which is generally an alpha source. The radioactive source was well-coated with the outer cladding material, thereby forming a cuboid heat source with four surfaces. The thermoelectric modules, whose number is the same as that of the peripheral surfaces of the heat source, were affixed to the source's surfaces and connected in series with each other. Each thermoelectric module consisted of four pairs of thermoelectric legs. Each thermocouple was composed of a P-type leg and an N-type leg with equivalent sizes. In Fig. 1, *L* and *S* indicate the length and the cross-sectional area of a single P-type or N-type leg, respectively. The internal holes and electrons of the PN thermocouples moved from the hot to the cold side. Electric current was then generated by the conducting electrodes. Finally, the output voltage of the RTG was released through the two electrodes.

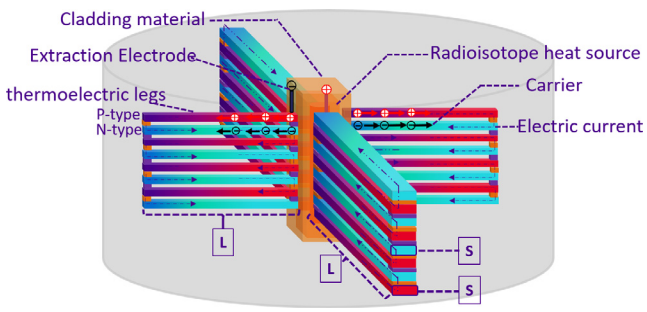

Fig. 1. Structure design of the radial RTG.

2.2. Preparation and testing

We intended to use a ^{241}Am isotope source and the bismuth telluride (Bi_2Te_3) thermoelectric module to produce a micro-radial RTG. The European Space Agency considers ^{241}Am as the preferred heat source of RTGs given its high specific heat power and long half-life (433a of half-life and 0.11 W/g of specific power) [26–28]. In the experiment, we adopted the method proposed by Scott A. Whalen et al. and used an electric heating rod of aluminum oxide (internal resistance of 3.2 Ω) as the simulated heat source [15,29,30]. As shown in Fig. 2(a), the Copper billet, which wrapped up the electric heating rod, was designed as an isotope source shielding material and a heat transfer layer. The total size of the heat source was $7 \times 7 \times 27\ mm^3$. The equivalent heat source could simulate the heat source power range of 0.1–1 W of the ^{241}Am source, and the corresponding source activities were 3.1–31.2 Ci.

The thermoelectric modules utilized Bi_2Te_3 as the thermoelectric material to achieve outstanding performance in the low-temperature section (shown in Table 1). First, the Bi_2Te_3 crystal rods were cut along the crystal growth direction into P- and N-type bulk materials using wire-electrode cutting. Both the P- and N- type legs were 10 mm length, 3 mm width, and 1 mm in height. Second, we performed electroplating and welding to join the four pairs of PN legs. Subsequently, a thermoelectric module connected to the ceramic was formed (see Fig. 2(b)). Third, the heat source and the four thermoelectric modules were put in a protective aluminum cylinder box. After that, the aluminum silicate cotton (1260-type) with a thermal conductivity of 0.03 W/(m·K) was placed in the box as a thermal insulation material. Finally, a micro-radial RTG was prepared as shown in Fig. 2(c).

The constant current for the electric heating rods was provided by a digital power source (Keithley 2231A). The RTG was tested

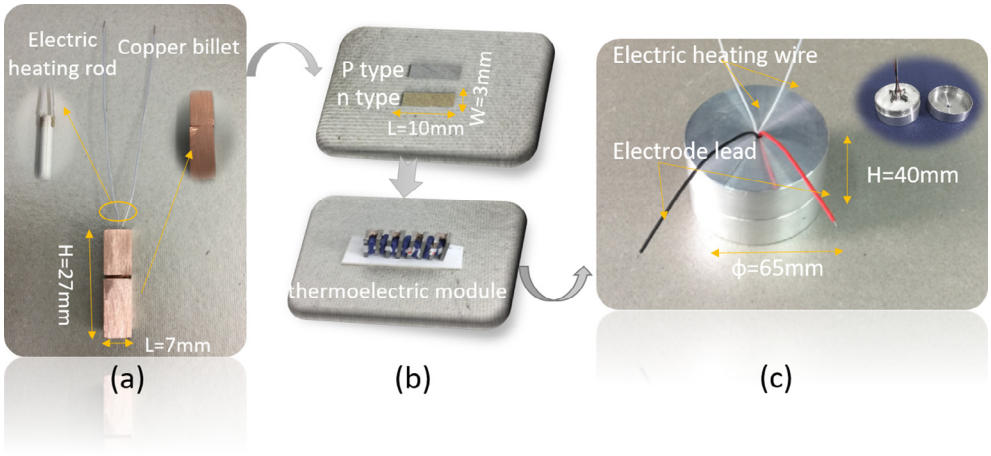

Fig. 2. Preparation process of a micro-radial RTG: (a) simulated heat source, (b) thermoelectric modules composed of 4-pair PN legs and (c) assembled RTG.

Table 1
Properties of Bi_2Te_3 thermoelectric materials used in the experiment.

Type	P-Type	n-Type
Density (g/cm^3)	6.8	7.8
Electrical conductivity σ (10^2 S/m)	2000~2600	2000~2600
Seebeck coefficient α (μV/K)	≥140	≥140
Thermal conductivity κ (W/ (m·K))	2.0~2.5	2.0~2.5
Power factor $\alpha^2\sigma$ (W/(m·K^2))	≥0.005	≥0.005
ZT value	≥0.7	≥0.7

using the dual channel digital source table (Keithley 2636A) for electrical performance output at an ambient temperature of 293.15 K. To minimize the error and improve the accuracy of the measurement data, the test was carried out after half an hour. At that time, the internal temperature of the RTG was stable. The LabTracer 2.9 software collected data and plotted the *I-V* characteristic curve, while the real-time temperatures of the hot and cold sides of the thermoelectric modules were measured by the temperature sensor (R7100). It is worth reminding that the temperature of the heat source can be approximately regarded as the hot end temperature of the thermoelectric module.

2.3. Finite element simulation

The relationship of the thermoelectric device's voltage, power, and size or structure was established theoretically for the three-dimensional model of the radial RTG in Fig. 1. The thermoelectric effect model of COMSOL software is used to simulate the process of converting thermal energy into electrical energy. The coupling analysis of heat transfer, current and thermoelectric effect was carried out. The equation of the relationship about the current density (J) and the heat flux (q) was given as follows:

$$-J = \sigma\nabla V + \sigma\alpha\nabla T \tag{1}$$

$$q = -\kappa\nabla T + T\alpha J \tag{2}$$

In steady state, the current density is was free to diverge, and the boundary condition can be expressed as follows:

$$\nabla \cdot J = 0 \tag{3}$$

$$q_0 = h(T_{ext} - T) \tag{4}$$

$$Q_{rad} = F_{12}A_1\varepsilon c(T_2^4 - T_1^4) \tag{5}$$

And at this moment the energy accumulation (Q) must be 0:

$$Q = \nabla \cdot (\kappa\nabla T) - \nabla((V + T\alpha) * J) = 0 \tag{6}$$

By solving the above equations and adopting the tetrahedral mesh generation method, the internal relations of potential V and temperature T with respect to the corresponding parameters such as conductivity, thermal conductivity, and size were established. Based the previous analysis, we discussed the steady-state output of the entire radial RTG. The output power (P_{out}), and the conversion efficiency (η) were calculated as follows [22]:

$$P_{out} = \frac{V^2}{(R+r)^2} \cdot R, \tag{7}$$

$$\eta = P_{out}/P_h \tag{8}$$

and

$$r = \frac{2\rho l}{S}.n \tag{9}$$

The open-circuit voltage (V_{oc}), which is the maximum value of the output voltage, is obtained when R is infinitely great. The maximum output power (P_{max}) and the maximum conversion efficiency (η_{max}) are obtained in Eqs. (8) and (9) when $R = r$. The analysis of the equations above suggests that the electrical output of the RTG was closely linked with the L and S of the thermoelectric legs and the value of n. Moreover, the electrical performance of the RTG can be improved considerably by optimizing these terms. Therefore, this research adopted the finite element analysis method to optimize the size of the thermocouple and the number of modules, thus establishing the variation curve between the output performance and the size or structure of RTGs. In this paper, we built a structural model of the RTG and set the heat source power in the solid heat transfer unit and electrical grounding in the current unit. Ultimately, the temperature field distribution and the electrical parameters like open-circuit voltage and internal resistance were obtained by coupling the solid heat transfer unit and current unit. The optimal output power of the RTG can be calculated by putting the open circuit voltage and internal resistance into the calculation formula of the article. Considering the RTG prototype was tested in an indoor environment, the air convection coefficient was set to 6 W/(m^2*K).

2.3.1. Size selection

According to Eqs. (7)–(9), the output performance of the micro-radial RTG is closely related to the size (including L and S) of the thermoelectric leg. To obtain an improved output, the length and cross-sectional area were optimized using the finite element

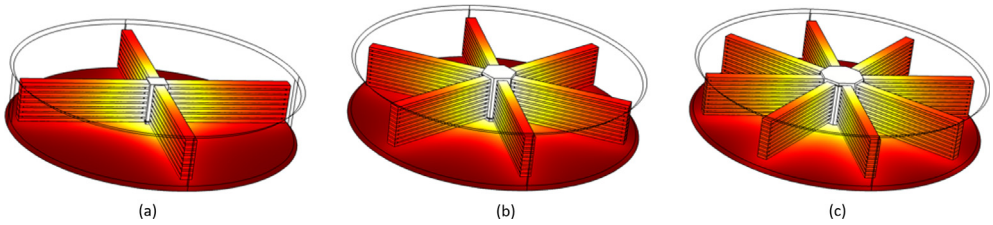

Fig. 3. RTGs with different numbers of modules: (a) four modules, (b) six modules and (c) eight modules.

simulation software COMOSOLCOMSOL. Considering the experimental parameters, L = 10 mm and S = 3 mm^2, the ranges of L and S were respectively set to 1–40 mm and 1.2–6 mm^2 during the simulation. The total cross-sectional area of all the thermoelectric legs for each module maintained a constant value (24 mm^2) during the entire optimization process. Furthermore, the heat sources changed from 0.1 W to 1 W in the optimization.

2.3.2. Thermoelectric module selection

Leg size was discussed previously for the micro-radial RTG based on four thermoelectric modules. Moreover, a micro-radial RTG could has other numbers of modules (for example, six or eight). In the study, we discussed the influence of the number of thermoelectric modules (four, six, and eight modules) on RTG. Our three thermoelectric structures with 4, 6, and 8 modules are shown in Fig. 3. The size of each thermocouple is based on the previously optimized dimensions. The same area of heat source surface was used for the three structures, that is, 5 × 20 mm^2. The RTG outputs were simulated at different heat source powers (0.1–1 W) to ascertain the preferred structure.

3. Results and discussion

3.1. Experimental test results

We first prepared the prototype sample of the RTG with the structure shown in Fig. 1 and then tested its performance. The external dimension of the prepared RTG is 65 mm (diameter) × 40 mm (height). The characteristic *I-V* curve of the RTG was measured by building a test platform for the electrical performance.

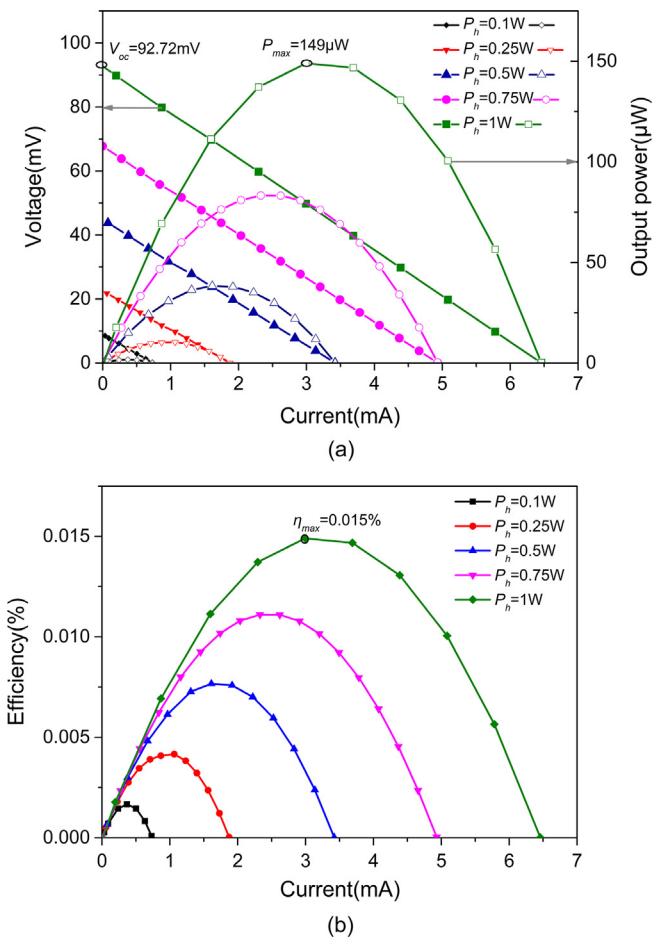

Fig. 4. (a) *I-V* characteristic curves and (b) conversion efficiency curves of the RTG under different heat source powers.

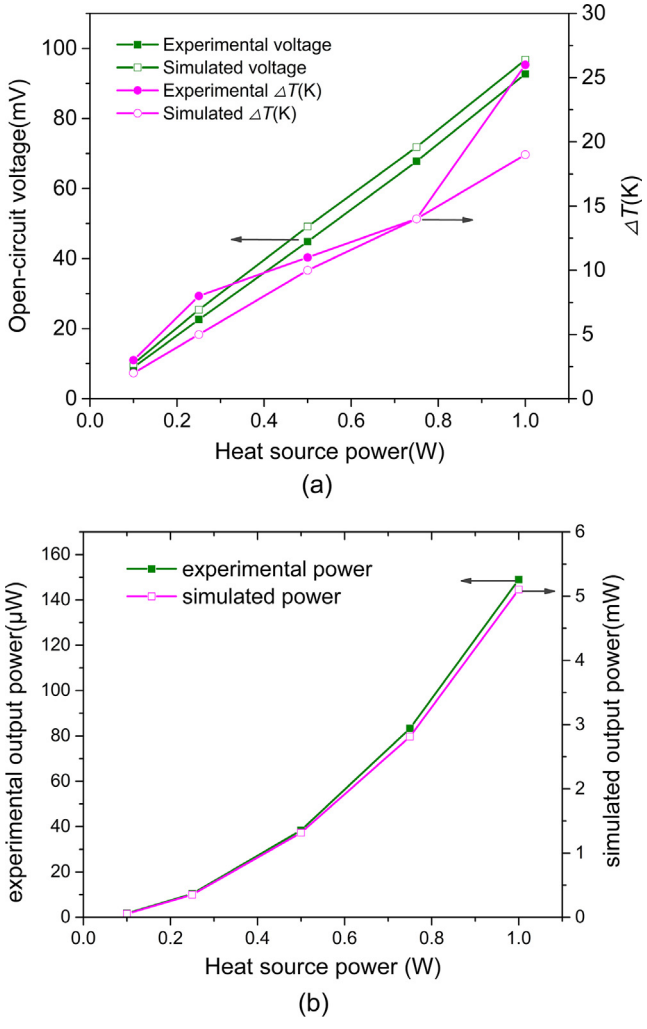

Fig. 5. Comparison of experimental and simulated values of the RTG: (a) open-circuit voltage and ΔT, (b) maximum output power.

The varying curve of the power P_{out} versus the current was obtained by multiplying the voltage with the current from the characteristic *I-V* curve. Fig. 4 displays the experimental output performances of the RTG at different heat source powers P_h. The output voltage is inversely proportional to the electric current. Additionally, the output power increased in the beginning and then decreased as the electric current increased. Both the output voltage and electric power increased with the rise of the heat source power. When the heat source power was 1 W, the entire RTG generated 92.72 mV open-circuit voltage (V_{oc}) and 149.0 μW maximum output power (P_{max}), which are the maximum values presented in Fig. 4(a). As shown in Fig. 4(b), the variation tendency of the conversion efficiency is similar to that of the output power of the RTG. The highest conversion efficiency η_{max} of 0.015%, which is the ratio of P_{max} divided by P_h, is a low value. During the actual preparation process, the poor contact between the electrode and the thermoelectric leg introduced a significant internal resistance. The test results show that the internal resistance of the RTG was 11.2 Ω at the ambient temperature of 293.15 K.

3.2. Simulation verification based on physical parameters of the prepared RTG

To verify the feasibility of the finite element analysis method, the COMSOL Multiphysics software was utilized to simulate the RTG using the same size and materials as the prepared sample. Fig. 5 shows the comparison of the experimental and simulated performances of the RTG. The measured V_{oc} values are very close to the simulation values. The simulated V_{oc} and P_{max} increased with the heat source power. This trend is similar to that of the measured V_{oc} and P_{max}. However, the simulated value is slightly larger than the measured one. The internal resistance of the RTG (11.2 Ω) is larger than the simulated value in COMSOL because the unprofessional welding level resulted in a large contact resistance in series. Moreover, the nonequivalent conditions, including material parameters and air convection, etc., also caused the difference between the simulation and the real experiment. The effect of the thermal insulation was worse than that in the simulation. This also explains the phenomenon wherein the simulated

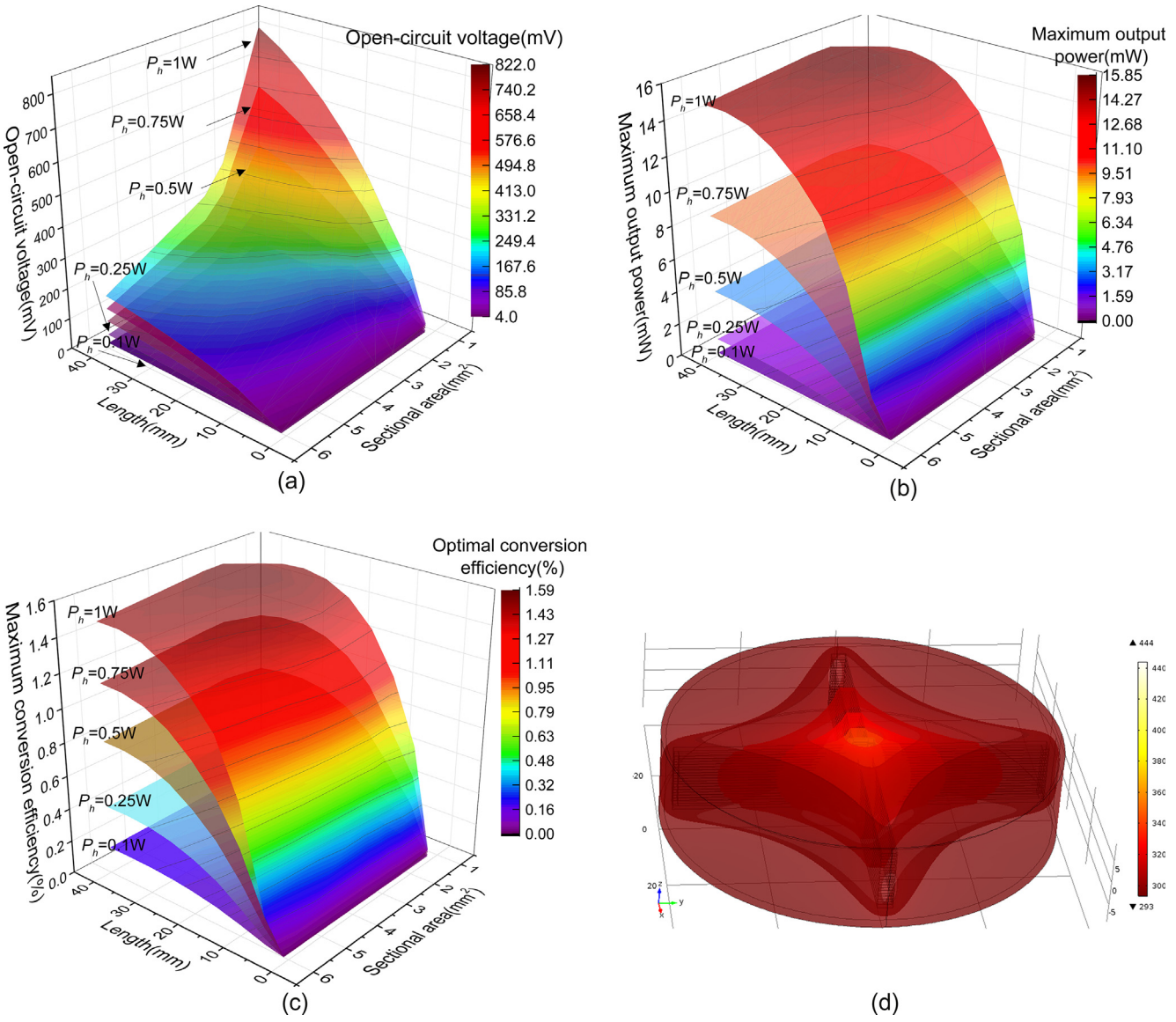

Fig. 6. Electrical output of the RTG under different sizes: (a) open-circuit voltage V_{oc}, (b) maximum output power P_{max}, (c) maximum conversion efficiency η and (d) the temperature distribution.

temperature difference between the two sides of the thermoelectric module was lower than the experimental value in Fig. 5(a). Their similarity is that the two temperature differences increased with the P_h. The power growth trends of both the experimental and simulated RTGs were highly consistent, although their output powers differ in Fig. 5(b) as the internal resistance of the experimental RTG increases. This difference can be reduced by improving the preparation process. Thus, the simulated electrical performance of the RTG was close to the measured value, thereby enabling the use of the finite element analysis software to simulate the thermoelectric conversion process accurately.

3.3. Optimization on the length and cross-sectional area of the thermoelectric leg

As shown in Fig. 6, the V_{oc}, the P_{max}, and the η_{max} of the micro-radial RTG were obtained by changing the values of L and S at different heat source powers. When the heat source powers increased, the values of V_{oc}, P_{max}, and η_{max} increased. In Fig. 6(a), the V_{oc} of the RTG increased with the increase of L and the decrease of S under the same heat source power. The elevated length of one thermoelectric leg led to large temperature differences at both sides. The number of thermocouples for the RTG increased as the S of an individual leg decreased due to the constant total cross-sectional area of all the thermoelectric legs. According to Eq. (1), the open-circuit voltage is equal to the product of the temperature difference and the number of thermocouples. Therefore, the V_{oc} get a large value at high L and small S. Thus, a maximum V_{oc} of 0.82 V was obtained with $L = 40$ mm and $S = 1.2$ mm^2 at the heat source power of 1 W.

As shown in Fig. 6(b) and (c), the maximum output power and the maximum conversion efficiency increased to peak values and then decreased with the increase of L and S. According to Eq. (2), internal resistance is another crucial factor that affects the performance of the RTG. The V_{oc} increased with L, consequently increasing the value of P_{max}. However, when L became long enough, the internal resistance r rose, consequently decreasing the value of P_{max}. As the value of S increased, the r of the RTG decreased, which increased P_{max}. However, when S becomes enough large, the number of thermocouples decreases. This brings down the value of V_{oc} and then reduced the value of P_{max}. Finally, the RTG achieved a maximum output power of 15.8 mW and a maximum conversion efficiency of 1.58% at $L = 35$ mm, $S = 2.4$ mm^2 and a heat source power of 1 W. The corresponding temperature distribution is shown in Fig. 6(d).

Table 2 shows the electrical performance of the micro-radial RTG before and after the optimization of the leg size and the comparison of the optimized and measured outputs at the same leg size. When we optimized the leg size from 10×3 mm^3 to 35×2.4 mm^3, the values of V_{oc}, P_{max}, and η_{max} increased significantly. A considerable gap exists between the simulated and measured values of P_{max} and η_{max}. As stated in Section 3.2, internal resistance mainly caused the gap. The results indicate that both the preparation process technology and the thermoelectric leg size should be improved in the future for the manufacture of micro-radial RTGs.

Table 2
Optimized and measured performance of the RTG at 1 W heat source power.

Leg dimension (L × S) (mm^3)	V_{oc} (mV)	P_{max} (mW)	η_{max} (%)
Simulated 35×2.4	402.24	15.8	1.58
Simulated 10×3	96.2	5.10	0.51
Measured 10×3	92.72	0.15	0.015

3.4. Influence of the number of thermoelectric modules on RTG

Fig. 7 shows the electrical performance of the RTG under different modules. The V_{oc} from the RTG with eight modules was highest, followed by that with six modules, and then by that with four modules under the same heat source power. The maximum value of V_{oc} was 474.5 mV. In terms of P_{max}, and η_{max}, the structure with four modules had the largest values, with 15.8 mW and 1.58% at a heat source power of 1 W.

When the thermoelectric modules increased from four to eight, the number of thermocouples rose remarkably. Subsequently, the open-circuit voltage increased. However, a large number of PN thermocouples also enhance internal resistance. At the same time, with the increase of the modules, the heat energy of each module can be reduced, and the consequent ΔT can also be reduced for a certain heat source power. Thus, V_{oc} increased as the number of modules increased. On the contrary, P_{max} and η_{max} decreased as the number of modules increased from four to eight. These results indicate that a substantial number of modules is recommended for a high open-circuit voltage, while a small number of modules is suggested for a high output power.

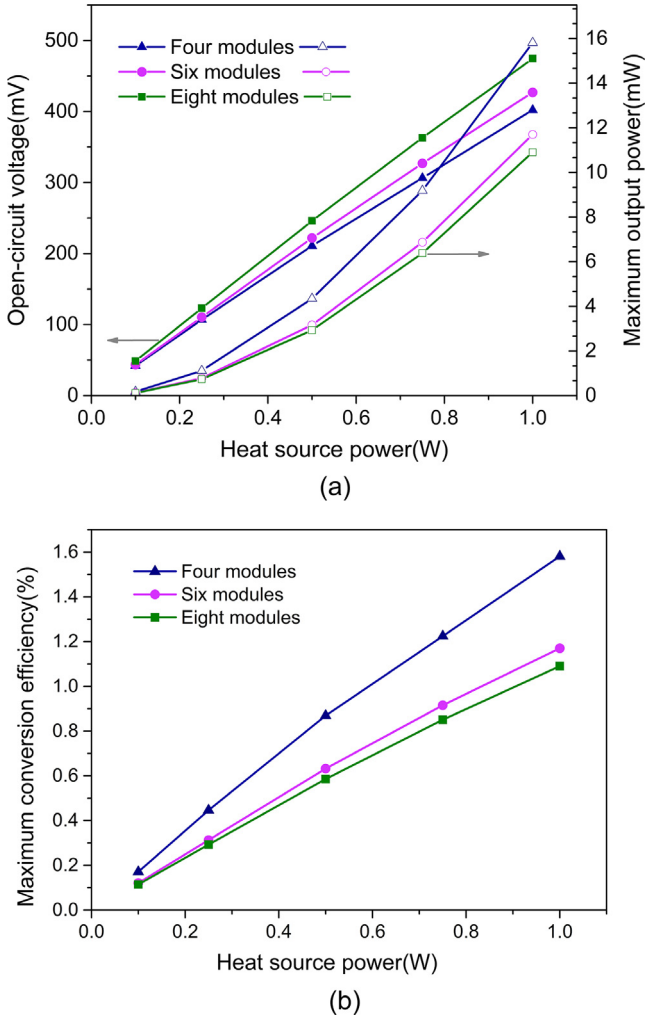

Fig. 7. Electrical performance of the RTG under different modules: (a) open-circuit voltage V_{oc} and maximum output power P_{max}, (b) maximum conversion efficiency η.

4. Conclusion

In this research, we designed and fabricated a micro-radial radioisotope thermoelectric generator. The relationship between the performance output and the structure size of the RTG was accurately established through theoretical analysis and simulation. A micro-radial RTG was experimentally fabricated, and its open-circuit voltage reached 92.72 mV at a heat source power of 1 W. The simulation data was suitably matched with the experimental results in terms of the output voltage and the temperature difference. The RTG with four thermoelectric modules, in which the size of a single thermoelectric leg was 35 mm length and 2.4 mm^2 cross-sectional area, was the best structural dimension at ambient temperature. The maximum output power of 15.8 mW was achieved when the heat source power was 1 W. The corresponding conversion efficiency was 1.58% at the heat source power of 1 W. Moreover, this study provides a feasible scheme for improving the output performance of a RTG by using the finite element analysis method properly. Future work should further enhance the preparation process technology and optimize the thermoelectric leg size in our manufactured micro-radial RTG toward realizing the RTG power supply for independent micro devices on spacecrafts in the near future.

Acknowledgements

This work was supported by the National Natural Science Foundation of China (Grant No. 11675076), the National Defense Basic Scientific Research Project (Grant No. JCKY2016605C006), the Natural Science Foundation of Jiangsu Province (Grant No. BK20150735), the Jiangsu Planned Projects for Postdoctoral Research Funds (Grant No. 1601139B), the Shanghai Aerospace Science and Technology Innovation Project (Grant No. SAST2016112), the Foundation of Graduate Innovation Center in NUAA (Grant No. kfjj20160609 and kfjj20170611), and the Priority Academic Program Development of Jiangsu Higher Education Institutions. Kai Liu and Yunpeng Liu have contributed equally to this work and should be regarded as co-first authors.

References

[1] M.A.G. Darrin, S.P. Buchner, M. Martin, The impact of the space radiation environment on micro electro mechanical systems (MEMS) and microstructures, radiation and its effects on components and systems, in: 8th European Conference on, IEEE, 2005, pp. H1-1-H1-5.
[2] J. Adams, D. Falconer, D. Fry, Q. Hu, G. Li, G.P. Zank, X. Ao, O. Verkhoglyadova, J. H. Adams, The ionizing radiation environment in space and its effects, AIP Conference Proceedings, vol. 1500, AIP, 2012, pp. 198–203.
[3] B. Russon, H. Tippets, G. Wilson, K. Gamaunt, A. Souvall, J. Dennison, Measurement of Effects of Long Term Ionizing Radiation on High Efficiency Solar Arrays, 2015.
[4] D.M. Rowe, CRC Handbook of Thermoelectrics, CRC Press, 1995.
[5] A. Pustovalov, Nuclear thermoelectric power units in Russia, USA and European space agency research programs, Proceedings ICT'97. XVI International Conference on. IEEE, 1997, pp. 559–562.
[6] P. Brooks, Final safety analysis ten-watt strontium-90 fueled generator for an unattended meteorological station. SNAP-7C, Martin Co. Nuclear Div., Baltimore, 1961.
[7] F. Ritz, C.E. Peterson, Multi-mission radioisotope thermoelectric generator (MMRTG) program overview, Aerospace Conference, vol. 5, IEEE, 2004, pp. 2950–2957.
[8] T. George, Overview of MEMS/NEMS Technology Development for Space Applications at NASA/JPL, Microtechnologies for the New Millennium 2003, International Society for Optics and Photonics, pp. 136–148.
[9] S.A. Jacobson, A.H. Epstein, An informal survey of power MEMS, Proc. ISMME K 18 (2003).
[10] A. Pustovalov, Mini-RTGs on plutonium-238: development and application, in: Eighteenth International Conference on. IEEE, 1999, pp. 509–520.
[11] G.R. Schmidt, R.L. Wiley, R.L. Richardson, R.R. Furlong, M.S. El-Genk, M.J. Bragg, NASA's program for radioisotope power system research and development, AIP Conference Proceedings, vol. 746, AIP, 2005, pp. 429–436.
[12] Y. Liu, X. Tang, Z. Xu, L. Hong, D. Chen, Experimental and theoretical investigation of temperature effects on an interbedded betavoltaic employing epitaxial Si and bidirectional 63 Ni, Appl. Radiat. Isotopes 94 (2014) 152–157.
[13] L. Hong, X.-B. Tang, Z.-H. Xu, Y.-P. Liu, D. Chen, Parameter optimization and experiment verification for a beta radioluminescence nuclear battery, J. Radioanal. Nucl. Chem. 302 (2014) 701–707.
[14] J. Weber, K. Potje-Kamloth, F. Haase, P. Detemple, F. Völklein, T. Doll, Coin-size coiled-up polymer foil thermoelectric power generator for wearable electronics, Sensors Actuators A: Phys. 132 (2006) 325–330.
[15] S.A. Whalen, C.A. Apblett, T.L. Aselage, Improving power density and efficiency of miniature radioisotopic thermoelectric generators, J. Power Sources 180 (2008) 657–663.
[16] X.D. Wang, Y.X. Huang, C.H. Cheng, D.T.W. Lin, C.H. Kang, A three-dimensional numerical modeling of thermoelectric device with consideration of coupling of temperature field and electric potential field, Energy 47 (2012) 488–497.
[17] J.H. Meng, X.X. Zhang, X.D. Wang, Multi-objective and multi-parameter optimization of a thermoelectric generator module, Energy 71 (2014) 367–376.
[18] J.H. Meng, X.X. Zhang, X.D. Wang, Characteristics analysis and parametric study of a thermoelectric generator by considering variable material properties and heat losses, Int. J. Heat Mass Transfer 80 (2015) 227–235.
[19] W.H. Chen, S.R. Huang, Y.L. Lin, Performance analysis and optimal operation of a thermoelectric generator by Taguchi method, Appl. Energy 158 (2015) 44–54.
[20] W.H. Chen, C.C. Wang, C.I. Hung, C.C. Yang, R.C. Juang, Modeling and simulation for the design of thermal-concentrated solar thermoelectric generator, Energy 64 (2014) 287–297.
[21] J. Chen, B. Lin, H. Wang, G. Lin, Optimal design of a multi-couple thermoelectric generator, Semicond. Sci. Technol. 15 (2000) 184.
[22] X. Jia, Y. Gao, Optimal design of a novel thermoelectric generator with linear-shaped structure under different operating temperature conditions, Appl. Therm. Eng. 78 (2015) 533–542.
[23] P. Aranguren, A. Roch, L. Stepien, et al., Optimized design for flexible polymer thermoelectric generators, Appl. Therm. Eng. 102 (2016) 402–411.
[24] A. Khajepour, F. Rahmani, An approach to design a 90Sr radioisotope thermoelectric generator using analytical and Monte Carlo methods with ANSYS COMSOL, and MCNP, Appl. Radiat. Isotopes 119 (2017) 51–59.
[25] B.L. Wang, A finite element computational scheme for transient and nonlinear coupling thermoelectric fields and the associated thermal stresses in thermoelectric materials, Appl. Therm. Eng. 110 (2017) 136–143.
[26] R. Ambrosi, H. Williams, P. Samara-Ratna, N. Bannister, D. Vernon, T. Crawford, C. Bicknell, A. Jorden, R. Slade, T. Deacon, Development and testing of Americium-241 radioisotope thermoelectric generator: concept designs and breadboard system, Nucl. Emerg. Technol. Space 3042 (2012).
[27] H. Williams, R. Ambrosi, N. Bannister, P. Samara-Ratna, J. Sykes, A conceptual spacecraft radioisotope thermoelectric and heating unit (RTHU), Int. J. Energy Res. 36 (2012) 1192–1200.
[28] R.C. O'Brien, R.M. Ambrosi, N.P. Bannister, et al., Safe radioisotope thermoelectric generators and heat sources for space applications, J. Nucl. Mater. 377 (3) (2008) 506–521.
[29] T.F. Hursen, S.A. Kolenik, Nuclear energy sources, Ann. N. Y. Acad. Sci. 167 (1969) 661–673.
[30] A. Pustovalov, V. Gusev, A. Borshchevsky, A. Chmielewski, Experimental confirmation of milliwatt power source concept, Eighteenth International Conference on, IEEE, 1999, pp. 500–504.